Published in final edited form as:
Biochim Biophys Acta. 2010 April ; 1803(4): 482–491. doi:10.1016/j.bbamcr.2009.12.006.

Redox signaling via lipid raft clustering in homocysteine-induced injury of podocytes

Chun Zhang, **Jun-Jun Hu**, **Min Xia**, **Krishna M. Boini**, **Christopher Brimson**, and **Pin-Lan Li**
Department of Pharmacology and Toxicology, Medical College of Virginia, Virginia Commonwealth University, Richmond, VA, 23298

Abstract

Our recent studies have indicated that hyperhomocysteinemia (hHcys) may induce podocyte damage, resulting in glomerulosclerosis. However, the molecular mechanisms mediating hHcys-induced podocyte injury are still poorly understood. In the present study, we first demonstrated that an intact NADPH oxidase system is present in podocytes as shown by detection of its membrane subunit ($gp91^{phox}$) and cytosolic subunit ($p47^{phox}$). Then, confocal microscopy showed that $gp91^{phox}$ and $p47^{phox}$ could be aggregated in lipid raft (LR) clusters in podocytes treated with homocysteine (Hcys), which were illustrated by their co-localization with cholera toxin B, a common LR marker. Different mechanistic LR disruptors, either methyl-β-cyclodextrin (MCD) or filipin abolished such Hcys-induced formation of LR-$gp91^{phox}$ or LR-$p47^{phox}$ transmembrane signaling complexes. By flotation of detergent-resistant membrane fractions we found that $gp91^{phox}$ and $p47^{phox}$ were enriched in LR fractions upon Hcys stimulation, and such enrichment of NADPH oxidase subunits and increase in its enzyme activity were blocked by MCD or filipin. Functionally, disruption of LR clustering significantly attenuated Hcys-induced podocyte injury, as shown by their inhibitory effects on Hcys-decreased expression of slit diaphragm molecules such as nephrin and podocin. Similarly, Hcys-increased expression of desmin was also reduced by disruption of LR clustering. In addition, inhibition of such LR-associated redox signaling prevented cytoskeleton disarrangement and apoptosis induced by Hcys. It is concluded that NADPH oxidase subunits aggregation and consequent activation of this enzyme through LR clustering is an important molecular mechanism triggering oxidative injury of podocytes induced by Hcys.

Keywords

Membrane microdomains; Oxidative injury; Homocysteine; Podocytes; Glomerulosclerosis

1. Introduction

Hyperhomocysteinemia (hHcys) has been known as an independent pathogenic factor in the progression of cardiovascular diseases [1–3]. There is also experimental evidence that homocysteine (Hcys) induces endothelial dysfunction, stimulates the proliferation of vascular

Send Correspondence and Reprint Requests to: Pin-Lan Li, MD, Ph.D, Department of Pharmacology and Toxicology, Medical College of Virginia Campus, Virginia Commonwealth University, 410 N. 12th Street, Richmond, VA 23298, Phone: (804)-828-4793, Fax: (804)-828-4794, pli@vcu.edu.

smooth muscle cells and disturbs the extracellular matrix metabolism [4–7]. These pathological changes constitute the molecular basis for the development of sclerotic process in vessel walls and other tissues [8]. In recent studies, we have reported that continuous hHcys could induce extracellular matrix accumulation in mesangial cells, which ultimately leads to glomerulosclerosis and causes the loss of renal function, resulting in end-stage renal disease [9–11]. Despite extensive studies, the precise mechanism mediating hHcys-induced glomerulosclerosis is still poorly understood. More recent studies in our laboratory and by others have shown that nicotinamide adenine dinucleotide phosphate (NADPH) oxidase activation and subsequent superoxide ($O_2^{\cdot-}$) generation importantly contribute to hHcys-induced glomerular injury [12,13]. However, it remains unknown how renal NADPH oxidase is activated by Hcys to produce local oxidative stress, in particular, how the subunits of this enzyme are aggregated or assembled in renal glomerular cells.

Podocytes are unique glomerular epithelial cells that comprise the outermost layer of the glomerular filtration barrier and serve as the final defense against urinary protein loss [14]. It has been reported that podocyte injury is an important early event leading to glomerulosclerosis in both genetic and non-genetic glomerular diseases [15]. Recently, we have demonstrated that hHcys may cause damages of podocytes and their slit diaphragm, leading to proteinuria and glomerulosclerosis [10]. However, it remains unknown whether hHcys-induced podocyte injury is associated with NADPH oxidase activation. In some recent studies, NADPH subunits were indeed detected in primarily cultured podocytes, which may mediate the pathogenic effects of high glucose- and angiotensin II-induced podocyte injury [16–18]. In the present study, we first characterized the expression and function of NADPH oxidase in a mouse podocyte cell line. Then, the mechanisms mediating NADPH oxidase activation in these podocytes in response to Hcys are explored. In such mechanistic studies, we focused on the possible driving force resulting in aggregation and assembling of NADPH oxidase subunits and thereby leading to its activation, which is associated with lipid raft (LR) clustering in the cell membrane of podocytes.

LRs are membrane lipid microdomains containing dynamic assemblies of cholesterol and lipids with saturated acyl chains such as sphingolipids and glycosphingolipids. These membrane LRs are able to cluster and thereby change their size, composition and specific protein-protein interactions upon various intra- or extra-cellular stimuli and result in the activation or amplification of signaling cascades [19,20]. The present hypothesis being tested to clarify NADPH activation in podocytes is that Hcys stimulates LR clustering, which drives aggregation and assembling of NADPH oxidase subunits to form a redox signaling platform or complex on podocyte membrane, whereby a local oxidative stress is produced and podocyte dysfunction and even apoptosis occur. A number of cellular and molecular approaches were used to test this hypothesis, and our results confirmed that LR clustering indeed plays a critical role in driving aggregation of NADPH oxidase subunits in podocytes, which results in $O_2^{\cdot-}$ production and subsequent podocyte injury.

2. Materials and methods

2.1. Cell culture

Conditionally immortalized mouse podocyte cell line was kindly provided by Dr. Paul E Klotman (Division of Nephrology, Department of Medicine, Mount Sinai School of Medicine, New York, USA). The cells were immortalized by a temperature-sensitive variant of the simian virus (SV40) which contains a large T antigen (tsA58) that is inducible by interferon–γ and stable at 33°C but rapidly degraded at 37°C [21]. At 33°C, the large T antigen allows for cellular proliferation. These cells were maintained on collagen-coated flasks or plates in RPMI 1640 medium supplemented with 10% fetal bovine serum, 10 units/ml recombinant mouse interferon–γ, 100U/ml penicillin and 100mg/ml streptomycin at 33°C. When the cells reached

confluence, they were passaged and allowed to differentiate at 37°C for 2 weeks without interferon–γ. Then, differentiated podocytes were used for experiments in different protocols as stated below. To determine the response of podocytes to high level of Hcys, L-Hcys, a pathogenic isoform of Hcys, was prepared and used as we and others described previously [22,23].

2.2. Animal procedures

To identify the expression of gp91^{phox} and p47^{phox} in mouse kidneys, 6-week old male C57BL/6J mice (Harlan Laboratories, Indianapolis, IN, USA) were used in this study. After anesthetized with 50 mg/kg pentobarbital intraperitoneally, the mice were sacrificed and the kidneys were excised. Then, the renal cortex were separated and saved for mRNA or protein detection. All animal protocols were approved by the Institutional Animal Care and Use Committee of Virginia Commonwealth University.

2.3. Real-time reverse transcription-polymerase chain reaction (RT-PCR)

Total RNA from podocytes or mouse renal cortex was isolated using TRIzol reagent (Invitrogen, Carlsbad, CA, USA) according to the protocol described by the manufacturer. RNA samples were quantified by measurement of optic absorbance at 260 nm and 280 nm in a spectrophotometer, with the A260/A280 ratio ranging from 1.8 to 2.0 which indicated a high purity of the extracted RNA. The concentrations of RNA were calculated by the intensity read at 260 nm. Aliquots of total RNA (1 μg) from each sample were reverse-transcribed into cDNA according to the instructions of the first strand cDNA synthesis kit of the manufacturer (Bio-Rad, Hercules, CA, USA). Equal amounts of the reverse transcriptional products were subjected to regular PCR amplification or using SYBR Green as fluorescence indicator on a Bio-Rad iCycler system (Bio-Rad, Hercules, CA, USA). The mRNA levels of target genes were normalized to the β-actin mRNA levels. The primers used in this study were synthesized by Operon (Huntsville, AL, USA) and the sequences were: gp91^{phox} sense TGGCACATCGATCCCTCACTGAAA, antisense GGTCACTGCATCTAAGGCAACCT; p47^{phox} sense GCCATCGAGGTCATTCATAA, antisense CTGCAGATACATGGATGGGA; nephrin sense CCCGGACACCTGTATGACGAG, antisense CCGCCACCTGGTCGTAGATT; podocin sense TGGCACATCGAT CCCTCACTGAAA, antisense AGGTCACTGCATCTAAGGCAACCT; desmin sense CAGTCCTACACCTGCGAGATT, antisense GGCCATCTTCACATTGAGC; β-actin sense TCGCTGCGCTGGTCGTC, antisense GGCCTCGTCACCCACATAGGA.

2.4. Immunocytochemistry detection of gp91^{phox} and p47^{phox} in podocytes

Immunocytochemistry was performed to determine the expression pattern of gp91^{phox} and p47^{phox} in differentiated podocytes. Podocytes were cultured in 4-well chambers. After the cells were washed with PBS, 4% PFA was used to fix the cells for 15 min. Then, the cells were washed with PBS and blocked with 1% bovine serum albumin (BSA) for 30 min. After washing with PBS, these cells were incubated with mouse anti-gp91^{phox} (1:50; BD biosciences, San Jose, CA, USA) or anti-p47^{phox} primary antibody (1:50; BD biosciences, San Jose, CA, USA) for 2 h at room temperature. After washing, the cells were incubated with goat-anti mouse IgG for 1 h. Then, the cells were incubated with streptavidin-HRP for 30 min at room temperature and stained with diaminobenzidine tetrahydrochloride (DAB) for 1 min. The slides were mounted and observed under a microscope in which photos were taken.

2.5. Confocal microscopic detection of LR and their colocalization with NADPH oxidase subunits in podocytes

For confocal microscopic detection of LR clusters and their associated proteins, podocytes were seeded on poly-L-lysine-coated chambers. The cells were treated with L-Hcys (80 μM,

a dose demonstrated to be most effective in inducing glomerular damage [22,23]) or vehicle for 30 min. In additional groups of cells, the LR disruptors, methyl-β-cyclodextrin (MCD) at 1 mM (Sigma, St. Louis, MO, USA) and filipin (1 μg/ml, Sigma, St. Louis, MO, USA), were added to pretreat cells for 30 min before addition of L-Hcys. LR clusters detection under confocal microscope was performed as previously described [24]. Briefly, podocytes were washed with cold PBS, fixed for 15 min in 4% paraformaldehyde (PFA) and then blocked with 1% BSA in PBS for 30 min. GM1 gangliosides enriched in LRs were stained with Alexa488-labeled cholera toxin B (Alexa488-CTXB) at 0.5 μg/mL (Molecular Probes, Eugene, OR, USA) for 30 min. For detection of the colocalization of LR and NADPH oxidase subunits gp91^{phox} and p47^{phox}, podocytes were incubated overnight with indicated primary monoclonal mouse anti-gp91^{phox} or anti-p47^{phox} at 1:100 (BD biosciences, San Jose, CA, USA) followed by incubation with 5 μg/mL Texas Red-conjugated anti-mouse IgG for an additional 1 h at room temperature. After mounting, the slides were observed using a confocal laser scanning microscope (Fluoview FV1000, Olympus, Japan). In each slide, the presence or absence of clustering in 100 cells was scored by an unwitting researcher after specifying the criteria for positive spots of fluorescence. Cells that displayed a homogenous distribution of fluorescence were indicated as negative. Results were given as the percentage of cells showing one or more overlaid fluorescent spots or patches in each protocol.

2.6. Flotation of membrane LR fractions

Podocytes pretreated with vehicle or filipin for 30 min were stimulated by addition of L-Hcys (80 μM) to the serum-free medium and incubated for 30 min. To isolate LR fractions from the cell membrane, these cells were lysed in 1.5 ml MBS buffer containing (in micromoles per liter) morpholinoethane sulfonic acid, 25; NaCl, 150; EDTA, 1; PMSF, 1; Na_3VO_4, 1; and a mixture of protease inhibitors and 1% Triton X-100 (pH 6.5). Cell extracts were homogenized by 5 passages through a 25-gauge needle. Then, homogenates were adjusted with 60% OptiPrep Density Gradient medium (Sigma, St. Louis, MO, USA) to 40% and overlaid with an equal volume (4.5 mL) of discontinuous 30%-5% OptiPrep Density Gradient medium. Samples were centrifuged at 32,000 rpm for 24 hours at 4°C using a SW32.1 rotor. Fractions were collected from the top to bottom. Then, these fractions were precipitated by mixing with an equal volume of 30% trichloroacetic acid and incubated for 30 min on ice. Precipitated proteins were spun down by centrifugation at 13,000 rpm at 4°C for 15 min. The protein pellet was carefully washed twice with cold acetone, air dried, and resuspended in 1 mol/L Tris-HCl (pH 8.0), which was then ready for Western blot analysis.

2.7. Western blot analysis

Western blot analysis was performed as we described previously [25]. In brief, proteins from the mouse renal cortex or cultured podocytes were extracted using sucrose buffer containing protease inhibitor. After boiled for 5 min at 95°C in a 5× loading buffer, 50 μg of total proteins or 25 μL of resuspended proteins (for detection of LR-associated proteins) were subjected to SDS-PAGE, transferred onto a PVDF membrane and blocked. Then, the membrane was probed with primary antibodies of anti-flotillin-1, a non-caveolar LR marker (1:1000, BD Biosciences, San Jose, CA), anti-gp91^{phox} (1:500, BD Biosciences, San Jose, CA), anti-p47^{phox} (1:500, BD Biosciences, San Jose, CA), anti-nephrin (1:500, Zymed, South San Francisco, CA, USA), anti-podocin (1:1000, Sigma, St. Louis, MO, USA), anti-desmin (1:1000, BD Biosciences, San Jose, CA, USA) or anti-β-actin (1:3000, Santa Cruz Biotechnology, Santa Cruz, CA, USA) overnight at 4°C followed by incubation with horseradish peroxidase–labeled IgG (1:5000). The immuno-reactive bands were detected by chemiluminescence methods and visualized on Kodak Omat X-ray films. Densitometric analysis of the images obtained from X-ray films was performed using the Image J software (NIH, Bethesda, MD, USA).

2.8. Electromagnetic spin resonance (ESR) analysis of $O_2^{\cdot -}$ production in podocytes

Podocytes pretreated with vehicle, apocynin (100 μM, a methoxy-substituted catechol that blocks NADPH oxidase assembly, but does not inhibit mitochondrial dehydrogenases [26]), MCD or filipin were incubated with L-Hcys (80μM) for 30 min. After treatment, cell proteins were extracted with a sucrose buffer and resuspended with modified Kreb's-Hepes buffer containing deferoximine (100 μM) and diethyldithiocarbamate (5 μM). The NADPH oxidase-dependent $O_2^{\cdot -}$ production was examined by addition of 1 mM NADPH as a substrate in 50 μg protein and incubated for 15 min at 37°C in the presence or absence of SOD (200 U/ml), and then supplied with 1 mM $O_2^{\cdot -}$ specific spin trap 1-hydroxy-3-methoxycarbonyl-2,2,5,5-tetramethylpyrrolidine (CMH, Sigma, St. Louis, MO, USA). The mixture was loaded in glass capillaries and immediately analyzed for $O_2^{\cdot -}$ production kinetically for 10 min. The ESR settings were as follows: biofield, 3350; field sweep, 60 G; microwave frequency, 9.78 GHz; microwave power, 20 mW; modulation amplitude, 3 G; 4,096 points of resolution; receiver gain, 20; and kinetic time, 10 min. The results were expressed as the fold changes vs. control group.

2.9. Direct fluorescence staining of F-actin

To determine the role of LR clustering and NADPH oxidase activation in Hcys-induced cytoskeleton changes, podocytes were cultured in 8-well chambers. After pretreatment with different inhibitors for 30 min, the cells were treated with L-Hcys (80 μM) or puromycin aminonucleoside (PAN, 100 μg/mL, Sigma, St. Louis, MO, USA) for 24 h. After washing with PBS, the cells were fixed in 4% paraformaldehyde for 15 min at room temperature, permeabilized with 0.1% Triton X-100, and blocked with 3% bovine serum albumin. F-actin was stained with rhodamine-phalloidin (Invitrogen, Carlsbad, CA, USA) for 15 min at room temperature. After mounting, the slides were examined by a confocal laser scanning microscope (Fluoview FV1000, Olympus, Japan). Cells with distinct F-actin fibers were counted as described previously [27]. Scoring was obtained from 100 podocytes on each slide in different groups.

2.10. Flow cytometry detection of podocyte apoptosis

The apoptosis rate of podocytes was detected using an Annexin V-propidiu iodide (PI) double staining kit (Sigma, St. Louis, MO, USA) according to the manufacturer's instructions. After the podocytes were pretreated with apocynin, MCD or filipin, the cells were incubated with L-Hcys (80 μM) for 48 h. PAN (100 μg/mL) was used to treat the cells for 48 h serving as a positive control to induce podocyte apoptosis. After treatment, podocytes were trypsinized and collected by centrifugation at 500 g for 8 min at room temperature. The cells were washed in cold (2–8°C) PBS and then subjected to another centrifugation. Then, the cells were resuspended in the Annexin V-PI reagent for 10 min at a concentration of 1×10^6 cells/100 μL. After washing with the reaction buffer and resuspension, the cells were detected using a flow cytometer (GUAVA, Hayward, CA, USA) within one hour.

2.11. Statistical Analysis

Data was presented as mean ± SEM. Significant differences among groups were assessed by one-way ANOVA test followed by a Duncan's multiple comparison post test using SigmaStat 3.5 software (Systat Software, Inc. Chicago, IL). χ^2 test was used to determine the significance of ratio and percentage data. $P<0.05$ was considered statistically significant.

3. Results

3.1. Characterization of gp91^{phox} and p47^{phox} expression in podocytes

Previous studies demonstrated that mRNA of NADPH oxidase subunits were detected in primarily cultured human podocytes [16], but the expression pattern of these subunits in mouse podocytes remains unknown. In the present study, we first examined the expression of two major NADPH oxidase subunits, gp91^{phox} and p47^{phox}, in a well-established mouse podocyte cell line. RT-PCR demonstrated that gp91^{phox} and p47^{phox} mRNAs were expressed in these cultured podocytes as well as in the normal mouse renal cortex which served as a positive control (Figure 1A). By Western blot and immunocytochemical analyses, we further confirmed the protein expression of these two NADPH oxidase subunits in podocytes (Figure 1B, 1C).

3.2. Colocalization of gp91^{phox} and p47^{phox} with LR clusters upon Hcys stimulation

To determine the association of gp91^{phox} and p47^{phox} with LRs, podocytes were stained with Alexa Fluo 488-labeled CTXB (a LR marker) and anti-gp91^{phox} or anti-p47^{phox} antibody to colocalize LRs and both NADPH oxidase subunits. As shown in Figure 2 and 3, CTXB was evenly distributed on the membrane of podocytes treated with vehicle (control). Upon stimulation with L-Hcys for 30 min, the LRs were detected by large and intense green fluorescent patches or spots, which were colocalized with gp91^{phox} or p47^{phox}. To explore whether these LR clusters are necessary for the recruitment of NADPH oxidase subunits, we observed the effect of two different LR disruptors, MCD and filipin, on Hcys-induced effect. It was found that both MCD and filipin significantly inhibited the colocalization of gp91^{phox} or p47^{phox} with LRs (Figure 2, Figure 3).

3.3. gp91^{phox} and p47^{phox} are enriched in isolated LR fractions upon Hcys stimulation

To further confirm the formation of LR-NADPH oxidase redox signaling complex, LR fractions were isolated and Western blot was performed to detect gp91^{phox} and p47^{phox}. As shown in Figure 4A, a positive expression of flotillin-1 was present in fractions 4 to 6, which suggested a successful isolation of LR fractions. gp91^{phox} could be detected in non-LR fractions from podocytes under normal condition. However, there was a marked increase of gp91^{phox} protein in LR fractions when cells were treated with Hcys. This increase was significantly inhibited by pretreatment with a lipid raft disruptor, filipin (Figure 4B). Although p47^{phox}, a cytosolic NADPH oxidase subunit, was not present in the LR fractions in control podocytes, it was found to be abundant in LR fractions upon L-Hcys stimulation, which was inhibited by filipin (Figure 4B). The summarized data is shown in Figure 4C.

3.4. NADPH oxidase inhibitor and LR disruptors block Hcys-induced $O_2^{\cdot-}$ production

Next, we analyzed NADPH oxidase-dependent $O_2^{\cdot-}$ generation in podocytes in the absence or presence of different inhibitors related to LR clustering and NADPH oxidase activity using ESR method. It was found that L-Hcys significantly increased NADPH oxidase-dependent $O_2^{\cdot-}$ generation (3.5 folds vs. control). This increased production of $O_2^{\cdot-}$ induced by L-Hcys was dramatically reduced when podocytes were pretreated with apocynin to inhibit the NADPH oxidase activity. More importantly, we found that two LR disruptors, MCD and filipin, also attenuated the increased $O_2^{\cdot-}$ production in podocytes induced by L-Hcys (Figure 5), suggesting that LR-associated NADPH oxidase is the main source of $O_2^{\cdot-}$ production upon L-Hcys stimulation.

3.5. Effects of NADPH oxidase inhibitors and LR disruptors on the expression of slit diaphragm molecules

To explore the functional relevance of LR clustering-associated NADPH oxidase activation, we examined the expression of two slit diaphragm molecules, nephrin and podocin, when

podocytes were incubated with L-Hcys in the absence or presence of NADPH oxidase inhibitors or LR disruptors. It was found that the mRNA levels of both nephrin and podocin were significantly decreased after treatment with L-Hcys for 12 h, which could be blocked by the pretreatment with NADPH oxidase inhibitors, diphenylene iodonium (DPI, 10μM) and apocynin (100μM), as well as with LR disruptors, MCD and filipin (Figure 6A). With a longer incubation time (24 h), the protein expressions of these molecules were decreased in a similar mode as mRNA expression (Figure 6B, 6C). However, a podocyte injury marker, desmin, was found increased when podocytes were treated with L-Hcys. Such increased desmin expression in podocytes treated with L-Hcys was substantially attenuated by either inhibition of NADPH oxidase or disruption of LRs (Figure 6).

3.6. Hcys-induced cytoskeleton disarrangement is recovered by NADPH oxidase inhibitor and LR disruptors

Under control conditions, most of the untreated podocytes showed distinct F-actin fibers along the longitudinal axis of these cells, as demonstrated by phalloidin-rhodamine staining. However, these fibers in podocytes treated with L-Hcys were reduced and reorganized to form peripheral fibers at the cell border. A similar pattern of F-actin redistribution was recapitulated by PAN treatment, which served as a positive control for inducing F-actin disarrangement in podocytes. When apocynin was used to inhibit the activity of NADPH oxidase, the F-actin staining was reversed to a normal pattern in L-Hcys-treated podocytes. Similarly, reduction and disarrangement of F-actin in these cells induced by L-Hcys was also prevented by MCD and filipin (Figure 7A). Summarized data in Figure 7B shows the ratio of cells retaining distinct F-actin fibers in different groups.

3.7. NADPH oxidase inhibitor and LR disruptors attenuate Hcys-induced podocyte apoptosis

Podocyte apoptosis is an important event initiating glomerulosclerosis. Although incubation of podocytes with L-Hcys (80 μM) for 24 h did not induce detectable apoptosis (data not shown), a prolonged incubation of these cells with L-Hcys (48 h) induced a marked apoptosis. We found that inhibition of NADPH oxidase using apocynin dramatically inhibited Hcys-induced podocyte apoptosis. Similarly, pretreatment of podocytes with LR disruptors, MCD and filipin, also protected them from Hcys-induced apoptosis (Figure 8).

4. Discussion

The major goal of the present study was to determine whether Hcys directly targets podocytes to induce their injury or dysfunction and to explore whether LR-associated redox signaling platforms play a critical role in Hcys-induced podocyte injury. Our results demonstrated that exposure of podocytes to Hcys caused significant injury of these cells as shown in changes in their structure and function such as reduced expression of slit diaphragm molecules, cytoskeleton disarrangement and cell apoptosis. It was also shown that such Hcys-induced podocyte injury was associated with the molecular trafficking and aggregation in LR clusters on the cell membrane, which resulted in assembling and activation of NADPH oxidase subunits leading to oxidative injury in these podocytes.

The NADPH oxidase family consists of membrane subunits gp91^{phox} and p22^{phox}, as well as cytosolic subunits p47^{phox}, p67^{phox} p40^{phox}, and *Rac*-1. Among these subunits, gp91^{phox} is the main catalytic and functional subunit, while p47^{phox} is cytosolic, serving as one of the most important regulatory subunits by translocation to cell membrane [28]. This NADPH oxidase has been shown to function in many types of mammalian cells to mediate redox regulation under physiological and pathological conditions [29–31]. However, little is known whether such redox enzyme is functioning in podocytes exposed to Hcys, even though there was a report that the mRNA of several NADPH oxidase subunits such as gp91^{phox}, p22^{phox}, p67^{phox} and

p47^{phox} could be detected in the primary cultures of human podocytes [16]. In the present study, we characterized the expression and function of this enzyme in murine podocytes and investigated the contribution of NADPH oxidase activation in mediating Hcys-induced podocyte injury. Indeed, we found that NADPH oxidase subunits are present in murine podocytes as shown by remarkable expression of gp91^{phox} and p47^{phox} mRNA and proteins. As measured by ESR, this NADPH oxidase produces $O_2^{\cdot-}$ and participates in the action of Hcys on podocyte structure and function.

Next, we tested how Hcys causes NADPH oxidase activation when it acts on podocytes. In this regards, it has long been accepted that the translocation and binding of p47^{phox} with membrane complex of gp91^{phox} and p22^{phox} are the key events leading to the activation of NADPH oxidase and generation of $O_2^{\cdot-}$ [32,33]. However, it remains unclear what is the determining factor, in particular, the driving force for the trafficking and aggregating of various NADPH oxidase subunits to the membrane of podocytes. Given the accumulating evidence showing that LR clustering is an early and rapid response to many pathological stimuli [19, 20,34], it is plausible that LR clustering on podocyte membrane may lead to aggregation and recruitment of NADPH oxidase subunits; thereby, forming redox platforms or signalosomes upon stimulation with Hcys. The present study did demonstrate that LR clustering is coupled to NADPH oxidase subunits aggregation on podocyte membrane in response to Hcys stimulation, as shown by gp91^{phox} and p47^{phox} colocalization with LRs on the cell membrane. Since p47^{phox} is normally located in the cytoplasma of cells, its detection on the cell membrane within LR clusters indicates possible trafficking and translocation of this subunit onto the cell membrane, which may be driven by LR clustering. This mechanism mediating NADPH oxidase aggregation or translocation was further confirmed by the use of LR disruptors. For example, treatment of podocytes with the cholesterol-sequestering agent, MCD, abolished this Hcys-induced colocalization of NADPH oxidase subunits with LRs and blocked NADPH oxidase-dependent $O_2^{\cdot-}$ production. Another lipid raft disruptor, filipin, which binds to cholesterol and disrupts the function of cholesterol-rich membrane, showed a similar effect to MCD. All these results support the view that Hcys activates LR clustering which leads to aggregation and assembling of NADPH oxidase subunits to form an active enzyme complex to produce $O_2^{\cdot-}$.

Furthermore, we isolated membrane LR fractions by flotation of detergent-resistant membrane preparations and confirmed that there was a marked increase in and gp91^{phox} and p47^{phox} proteins in LR fractions when podocytes were exposed to Hcys. This increase in NADPH oxidase subunits was abolished by a LR disruptor, filipin. These results further confirm a rapid shift of these NADPH oxidase subunits between LR and non-LR fractions in the cell membrane when podocytes were challenged by Hcys. It is the clustering of LRs that provide the driving force for the recruitment of NADPH oxidase subunits such as p47^{phox} to activate this enzyme and form a redox signaling platform within the podocyte membrane.

To explore the functional relevance of LR redox signaling platforms in Hcys-induced podocyte injury, we detected the expression of podocyte slit diaphragm molecules, nephrin and podocin upon stimulation with Hcys. In this regard, the slit diaphragm between the neighbored foot processes of podocytes has an important and direct role in regulating glomerular filtration and preventing the leakage of plasma proteins [35]. Slit diaphragm proteins such as nephrin and podocin have been reported to contribute to the regulation of cell polarity, cell survival and cytoskeletal organization [36]; therefore, reduction of these slit diaphragm proteins may result in glomerular injury or sclerosis [37,38]. The present study demonstrated that the expression of nephrin and podocin was suppressed by Hcys both at mRNA and protein levels, which was restored by NADPH oxidase inhibitors. This decreased expression of nephrin and podocin was contrasted by an increase in desmin, a podocyte injury factor. These results were consistent with our previous results from an *in vivo* hHcys animal model [10], suggesting that Hcys may

cause podocyte damage by interfering with the composition and function of the slit diaphragm. Importantly, both a decrease in slit diaphragm proteins and an increase in desmin in podocytes induced by Hcys were found to be blocked by inhibition of LR clustering. Taken together, these results demonstrate that Hcys may cause slit diaphragm disruption and subsequent podocyte injury through LR-NADPH oxidase signaling platforms.

In differentiated podocytes, the actin cytoskeleton is organized into fibroblast-like stress fibers extending into the foot processes, comparable to that of smooth muscle cells or pericytes [21]. It has been assumed that stress fibers in cultured podocytes correspond to the filamentous actin in podocyte foot processes *in vivo* and as such represent differentiation of podocytes [39]. Foot process effacement, the hallmark of podocyte injury and proteinuric kidney disease, is often accompanied by the disruption of these well-aligned filaments. It is now widely accepted that stress fibers reflect various changes in intracellular signaling pathways and actin dynamics is one of the useful tools in evaluating the functional changes of podocytes, especially when combined with other markers. In the present study, we found that Hcys induced a dramatic disarrangement of F-actin, which was comparable to a classic podocyte damage inducer, PAN. Inhibition of NADPH oxidase activity and disruption of LR clustering substantially blocked this Hcys-induced actin filament disarrangement. These results together with the changes in the slit diaphragm molecules upon Hcys strengthened the important role of LRs in inducing podocyte dysfunction by recruiting and activating NADPH oxidase and subsequent generation of $O_2^{\cdot-}$.

It has been reported that depletion of podocytes in the glomeruli is the strongest predictor for the progression of glomerulosclerosis, where fewer cells predict more rapid progression [40]. Recently, it has been demonstrated that podocyte apoptosis is a key mechanism leading to podocyte loss in diabetic nephropathy [41], PAN-induced nephrosis [42], and transgenic mice expressing transforming growth factor-β1 (TGF-β1) [43]. Until now, there is no evidence to show whether Hcys could cause apoptosis in podocytes. Our cytometric analysis showed that with a prolonged incubation time (48 h), Hcys increased the rate of podocyte apoptosis by 4 folds compared to vehicle-treated cells, which was blocked or attenuated by inhibition of NADPH oxidase or LR clustering. Since podocytes are terminally differentiated cells *in vivo* with a limited capacity to proliferate, it seems that LR clustering and consequent activation of NADPH oxidase importantly contribute to podocyte loss and subsequent glomerulosclerosis associated with hHcys through its action to induce apoptosis.

In summary, the present study demonstrates a novel mechanism of Hcys-induced podocyte injury, which may represent an early event initiating glomerulosclerosis during hHcys. This mechanism is characterized by the clustering of membrane LRs, recruitment and assembling of NADPH oxidase subunits, production of $O_2^{\cdot-}$ and functional disturbance in podocytes. Therefore, LR clustering as an early event in the cascade of podocyte apoptosis and glomerulosclerosis may be a target for the development of therapeutic strategy for treatment and prevention of hHcys-induced end-stage renal disease associated with hypertension, diabetes or aging.

Acknowledgments

This study was supported by grants DK54927, HL075316, and HL57244 from National Institutes of Health.

References

1. Robinson K, Gupta A, Dennis V, Arheart K, Chaudhary D, Green R, Vigo P, Mayer EL, Selhub J, Kutner M, Jacobsen DW. Hyperhomocysteinemia confers an independent increased risk of atherosclerosis in end-stage renal disease and is closely linked to plasma folate and pyridoxine concentrations. Circulation 1996;94:2743–2748. [PubMed: 8941098]

2. Moustapha A, Gupta A, Robinson K, Arheart K, Jacobsen DW, Schreiber MJ, Dennis VW. Prevalence and determinants of hyperhomocysteinemia in hemodialysis and peritoneal dialysis. Kidney Int 1999;55:1470–1475. [PubMed: 10201012]
3. Ducloux D, Motte G, Challier B, Gibey R, Chalopin JM. Serum total homocysteine and cardiovascular disease occurrence in chronic, stable renal transplant recipients: a prospective study. J. Am. Soc. Nephrol 2000;11:134–137. [PubMed: 10616849]
4. Chow K, Cheung F, Lao TT, O K. Effect of homocysteine on the production of nitric oxide in endothelial cells. Clin. Exp. Pharmacol. Physiol 1999;26:817–818. [PubMed: 10549408]
5. Erol A, Cinar MG, Can C, Olukman M, Ulker S, Kosay S. Effect of homocysteine on nitric oxide production in coronary microvascular endothelial cells. Endothelium 2007;14:157–161. [PubMed: 17578710]
6. Liu X, Luo F, Li J, Wu W, Li L, Chen H. Homocysteine induces connective tissue growth factor expression in vascular smooth muscle cells. J. Thromb. Haemost 2008;6:184–192. [PubMed: 17944991]
7. Guo H, Lee JD, Uzui H, Yue H, Wang P, Toyoda K, Geshi T, Ueda T. Effects of heparin on the production of homocysteine-induced extracellular matrix metalloproteinase-2 in cultured rat vascular smooth muscle cells. Can. J. Cardiol 2007;23:275–280. [PubMed: 17380220]
8. Papatheodorou L, Weiss N. Vascular oxidant stress and inflammation in hyperhomocysteinemia. Antioxid. Redox Signal 2007;9:1941–1958. [PubMed: 17822365]
9. Yi F, Chen QZ, Jin S, Li PL. Mechanism of homocysteine-induced Rac1/NADPH oxidase activation in mesangial cells: role of guanine nucleotide exchange factor Vav2. Cell. Physiol. Biochem 2007;20:909–918. [PubMed: 17982273]
10. Yi F, dos Santos EA, Xia M, Chen QZ, Li PL, Li N. Podocyte injury and glomerulosclerosis in hyperhomocysteinemic rats. Am. J. Nephrol 2007;27:262–268. [PubMed: 17396029]
11. Yi F, Li PL. Mechanisms of homocysteine-induced glomerular injury and sclerosis. Am. J. Nephrol 2008;28:254–264. [PubMed: 17989498]
12. Yi F, Xia M, Li N, Zhang C, Tang L, Li PL. Contribution of guanine nucleotide exchange factor Vav2 to hyperhomocysteinemic glomerulosclerosis in rats. Hypertension 2009;53:90–96. [PubMed: 19029489]
13. Sen U, Basu P, Abe OA, Givvimani S, Tyagi N, Metreveli N, Shah KS, Passmore JC, Tyagi SC. Hydrogen sulfide ameliorates hyperhomocysteinemia-associated chronic renal failure. Am. J. Physiol. Renal Physiol 2009;297:F410–F419. [PubMed: 19474193]
14. Ortiz A, Marron B, Ramos A. The fate of podocytes in proteinuric nephropathies. Nefrologia 2002;22:425–431. [PubMed: 12497743]
15. Tryggvason K, Patrakka J, Wartiovaara J. Hereditary proteinuria syndromes and mechanisms of proteinuria. N. Engl. J. Med 2006;354:1387–1401. [PubMed: 16571882]
16. Greiber S, Munzel T, Kastner S, Muller B, Schollmeyer P, Pavenstadt H. NAD(P)H oxidase activity in cultured human podocytes: effects of adenosine triphosphate. Kidney Int 1998;53:654–663. [PubMed: 9507211]
17. Eid AA, Gorin Y, Fagg BM, Maalouf R, Barnes JL, Block K, Abboud HE. Mechanisms of podocyte injury in diabetes: role of cytochrome P450 and NADPH oxidases. Diabetes 2009;58:1201–1211. [PubMed: 19208908]
18. Whaley-Connell AT, Chowdhury NA, Hayden MR, Stump CS, Habibi J, Wiedmeyer CE, Gallagher PE, Tallant EA, Cooper SA, Link CD, Ferrario C, Sowers JR. Oxidative stress and glomerular filtration barrier injury: role of the renin-angiotensin system in the Ren2 transgenic rat. Am. J. Physiol. Renal Physiol 2006;291:F1308–F1314. [PubMed: 16788142]
19. Simons K, Ikonen E. Functional rafts in cell membranes. Nature 1997;387:569–572. [PubMed: 9177342]
20. Simons K, Toomre D. Lipid rafts and signal transduction. Nat. Rev. Mol. Cell. Biol 2000;1:31–39. [PubMed: 11413487]
21. Mundel P, Reiser J, Zuniga Mejia Borja A, Pavenstadt H, Davidson GR, Kriz W, Zeller R. Rearrangements of the cytoskeleton and cell contacts induce process formation during differentiation of conditionally immortalized mouse podocyte cell lines. Exp. Cell. Res 1997;236:248–258. [PubMed: 9344605]

22. Yi F, Zhang AY, Janscha JL, Li PL, Zou AP. Homocysteine activates NADH/NADPH oxidase through ceramide-stimulated Rac GTPase activity in rat mesangial cells. Kidney Int 2004;66:1977–1987. [PubMed: 15496169]

23. Qureshi I, Chen H, Brown AT, Fitzgerald R, Zhang X, Breckenridge J, Kazi R, Crocker AJ, Stuhlinger MC, Lin K, Cooke JP, Eidt JF, Moursi MM. Homocysteine-induced vascular dysregulation is mediated by the NMDA receptor. Vasc. Med 2005;10:215–223. [PubMed: 16235775]

24. Jia SJ, Jin S, Zhang F, Yi F, Dewey WL, Li PL. Formation and function of ceramide-enriched membrane platforms with CD38 during M1-receptor stimulation in bovine coronary arterial myocytes. Am. J. Physiol. Heart Circ. Physiol 2008;295:H1743–H1752. [PubMed: 18723763]

25. Zhang DX, Zou AP, Li PL. Ceramide-induced activation of NADPH oxidase and endothelial dysfunction in small coronary arteries. Am. J. Physiol. Heart Circ. Physiol 2003;284:H605–H612. [PubMed: 12424096]

26. Touyz RM. Apocynin, NADPH oxidase, and vascular cells: a complex matter. Hypertension 2008;51:172–174. [PubMed: 18086948]

27. Yang L, Zheng S, Epstein PN. Metallothionein over-expression in podocytes reduces adriamycin nephrotoxicity. Free Radic. Res 2009;43:174–182. [PubMed: 19204870]

28. Vignais PV. The superoxide-generating NADPH oxidase: structural aspects and activation mechanism. Cell. Mol. Life Sci 2002;59:1428–1459. [PubMed: 12440767]

29. Poinas A, Gaillard J, Vignais P, Doussiere J. Exploration of the diaphorase activity of neutrophil NADPH oxidase. Eur. J. Biochem 2002;269:1243–1252. [PubMed: 11856358]

30. Mohazzab KM, Kaminski PM, Wolin MS. NADH oxidoreductase is a major source of superoxide anion in bovine coronary artery endothelium. Am. J. Physiol 1994;266:H2568–H2572. [PubMed: 8024019]

31. Meier B, Jesaitis AJ, Emmendorffer A, Roesler J, Quinn MT. The cytochrome b-558 molecules involved in the fibroblast and polymorphonuclear leucocyte superoxide-generating NADPH oxidase systems are structurally and genetically distinct. Biochem. J 1993;289(Pt 2):481–486. [PubMed: 7678734]

32. Castier Y, Brandes RP, Leseche G, Tedgui A, Lehoux S. p47phox-dependent NADPH oxidase regulates flow-induced vascular remodeling. Circ. Res 2005;97:533–540. [PubMed: 16109921]

33. Zhang G, Zhang F, Muh R, Yi F, Chalupsky K, Cai H, Li PL. Autocrine/paracrine pattern of superoxide production through NAD(P)H oxidase in coronary arterial myocytes. Am. J. Physiol. Heart Circ. Physiol 2007;292:H483–H495. [PubMed: 16963617]

34. Peshavariya H, Dusting GJ, Di Bartolo B, Rye KA, Barter PJ, Jiang F. Reconstituted high-density lipoprotein suppresses leukocyte NADPH oxidase activation by disrupting lipid rafts. Free Radic. Res 2009:1–11.

35. Kawachi H, Miyauchi N, Suzuki K, Han GD, Orikasa M, Shimizu F. Role of podocyte slit diaphragm as a filtration barrier. Nephrology (Carlton) 2006;11:274–281. [PubMed: 16889564]

36. Huber TB, Benzing T. The slit diaphragm: a signaling platform to regulate podocyte function. Curr. Opin. Nephrol. Hypertens 2005;14:211–216. [PubMed: 15821412]

37. Endlich N, Kress KR, Reiser J, Uttenweiler D, Kriz W, Mundel P, Endlich K. Podocytes respond to mechanical stress in vitro. J. Am. Soc. Nephrol 2001;12:413–422. [PubMed: 11181788]

38. Uchida K, Suzuki K, Iwamoto M, Kawachi H, Ohno M, Horita S, Nitta K. Decreased tyrosine phosphorylation of nephrin in rat and human nephrosis. Kidney Int 2008;73:926–932. [PubMed: 18256598]

39. Mundel P, Shankland SJ. Podocyte biology and response to injury. J. Am. Soc. Nephrol 2002;13:3005–3015. [PubMed: 12444221]

40. Shankland SJ. The podocyte's response to injury: role in proteinuria and glomerulosclerosis. Kidney Int 2006;69:2131–2147. [PubMed: 16688120]

41. Isermann B, Vinnikov IA, Madhusudhan T, Herzog S, Kashif M, Blautzik J, Corat MA, Zeier M, Blessing E, Oh J, Gerlitz B, Berg DT, Grinnell BW, Chavakis T, Esmon CT, Weiler H, Bierhaus A, Nawroth PP. Activated protein C protects against diabetic nephropathy by inhibiting endothelial and podocyte apoptosis. Nat. Med 2007;13:1349–1358. [PubMed: 17982464]

42. Koshikawa M, Mukoyama M, Mori K, Suganami T, Sawai K, Yoshioka T, Nagae T, Yokoi H, Kawachi H, Shimizu F, Sugawara A, Nakao K. Role of p38 mitogen-activated protein kinase

activation in podocyte injury and proteinuria in experimental nephrotic syndrome. J. Am. Soc. Nephrol 2005;16:2690–2701. [PubMed: 15987752]

43. Schiffer M, Bitzer M, Roberts IS, Kopp JB, ten Dijke P, Mundel P, Bottinger EP. Apoptosis in podocytes induced by TGF-beta and Smad7. J. Clin. Invest 2001;108:807–816. [PubMed: 11560950]

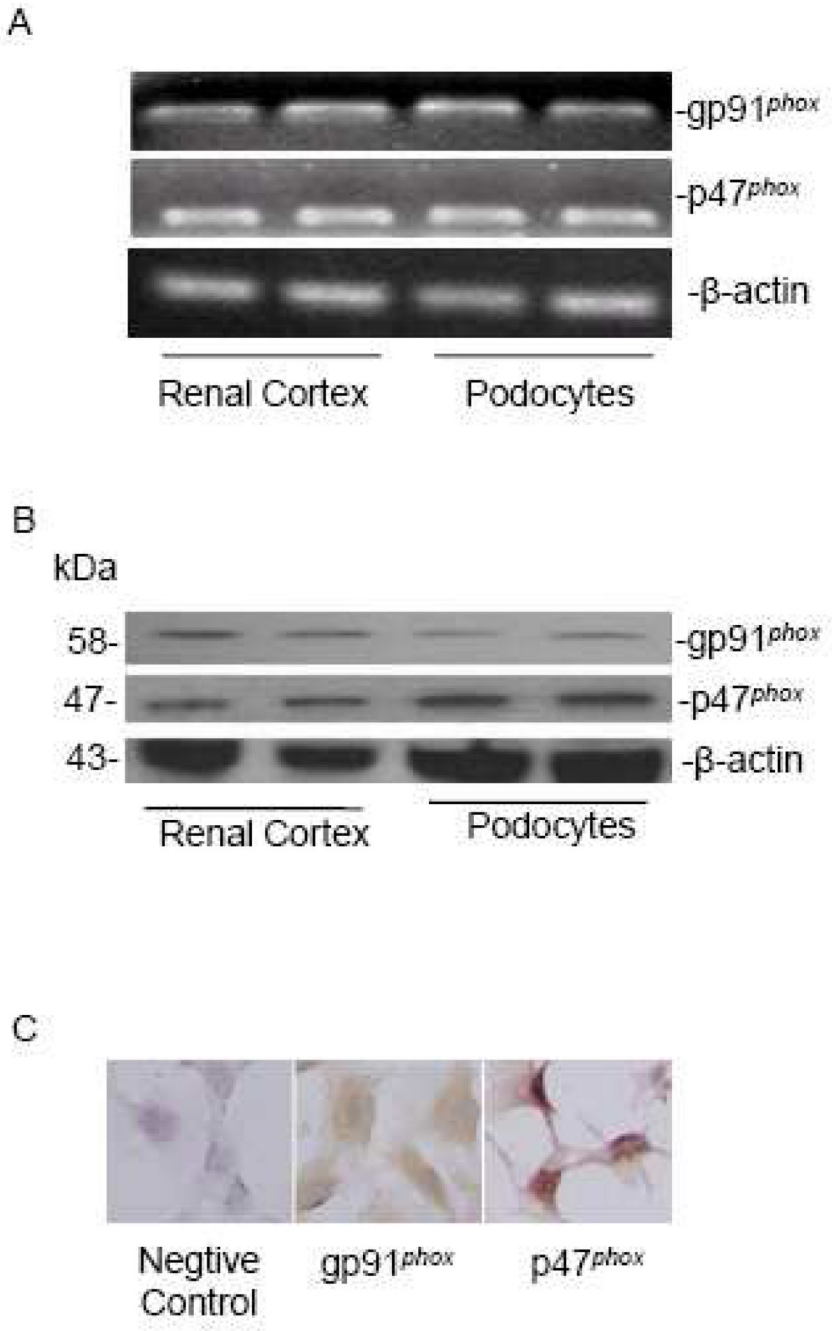

Figure 1. gp91*phox* and p47*phox* are present in murine podocytes

A: A representative gel image shows mRNA expression of gp91*phox* and p47*phox* in mice renal cortex and podocytes (RT-PCR); B: Western blot analysis of gp91*phox* and p47*phox* in the renal cortex and podocytes; C: Immunocytochemistry staining of gp91*phox* and p47*phox* in podocytes (Original magnification, ×400).

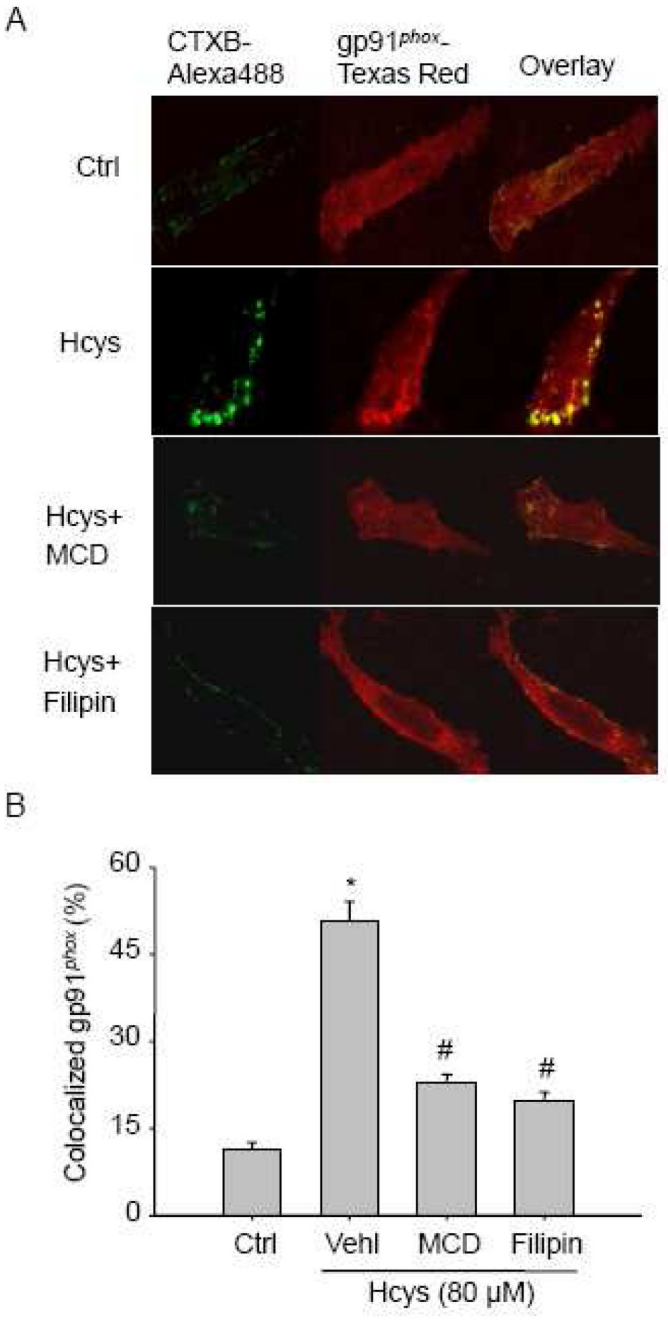

Figure 2. Hcys induces LR-gp91*phox* clustering in podocytes, which is blocked by LR disruptors

A. Representative confocal microscopic images of LR-gp91*phox* clusters in podocytes. Alexa-488-CTXB is shown as a green color on the left; Texas Red-conjugated gp91*phox* as a red color in the middle; and the overlaid images on the right. Yellow spots or patches in the overlaid images were defined as LR-gp91*phox* clusters (Original magnification, ×1000). B. Summarized data shows the effect of Hcys on the formation of LR-gp91*phox* clusters in the presence or absence of LR disruptors. Panel bars mean values ± SEM of 5 experiments with the analysis of 100 podocytes on each slide. Ctrl: control; Vehl: vehicle. * $P<0.05$ vs. control; # $P<0.05$ vs. Hcys.

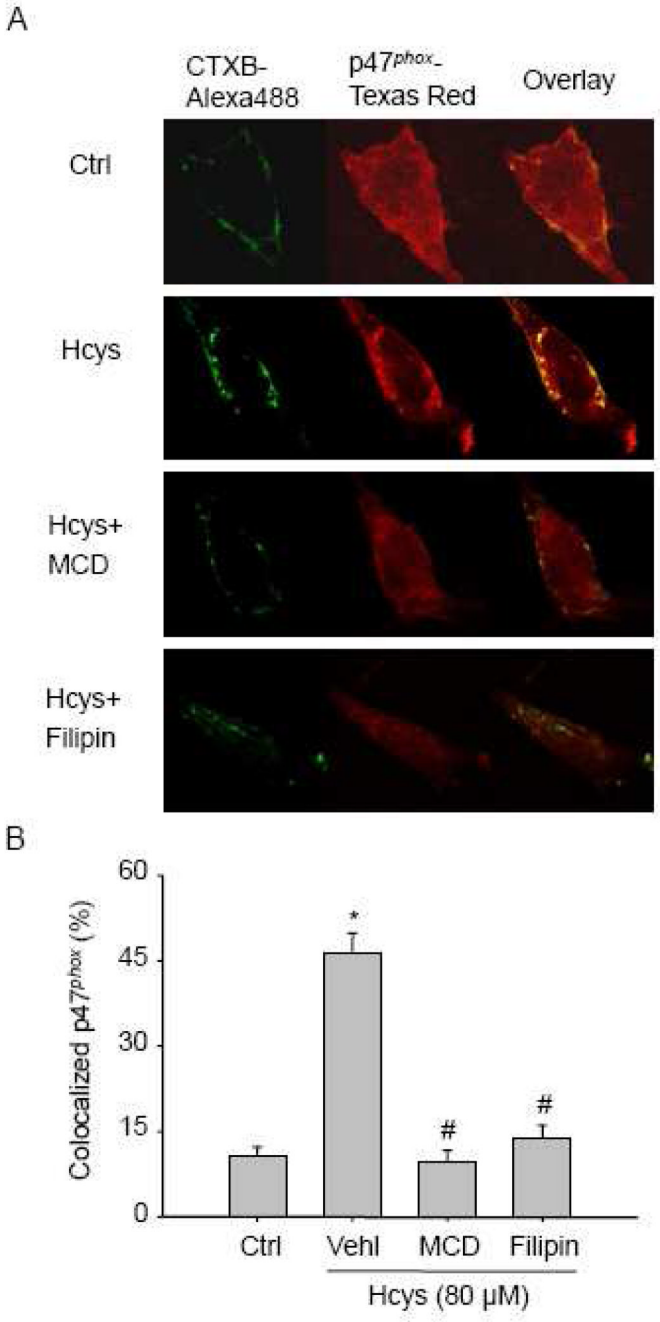

Figure 3. Hcys induces LR-p47*phox* clustering in podocytes, which is blocked by LR disruptors

Description of panels is the same as those in Figures 2 except that p47*phox* was substituted for gp91*phox*.

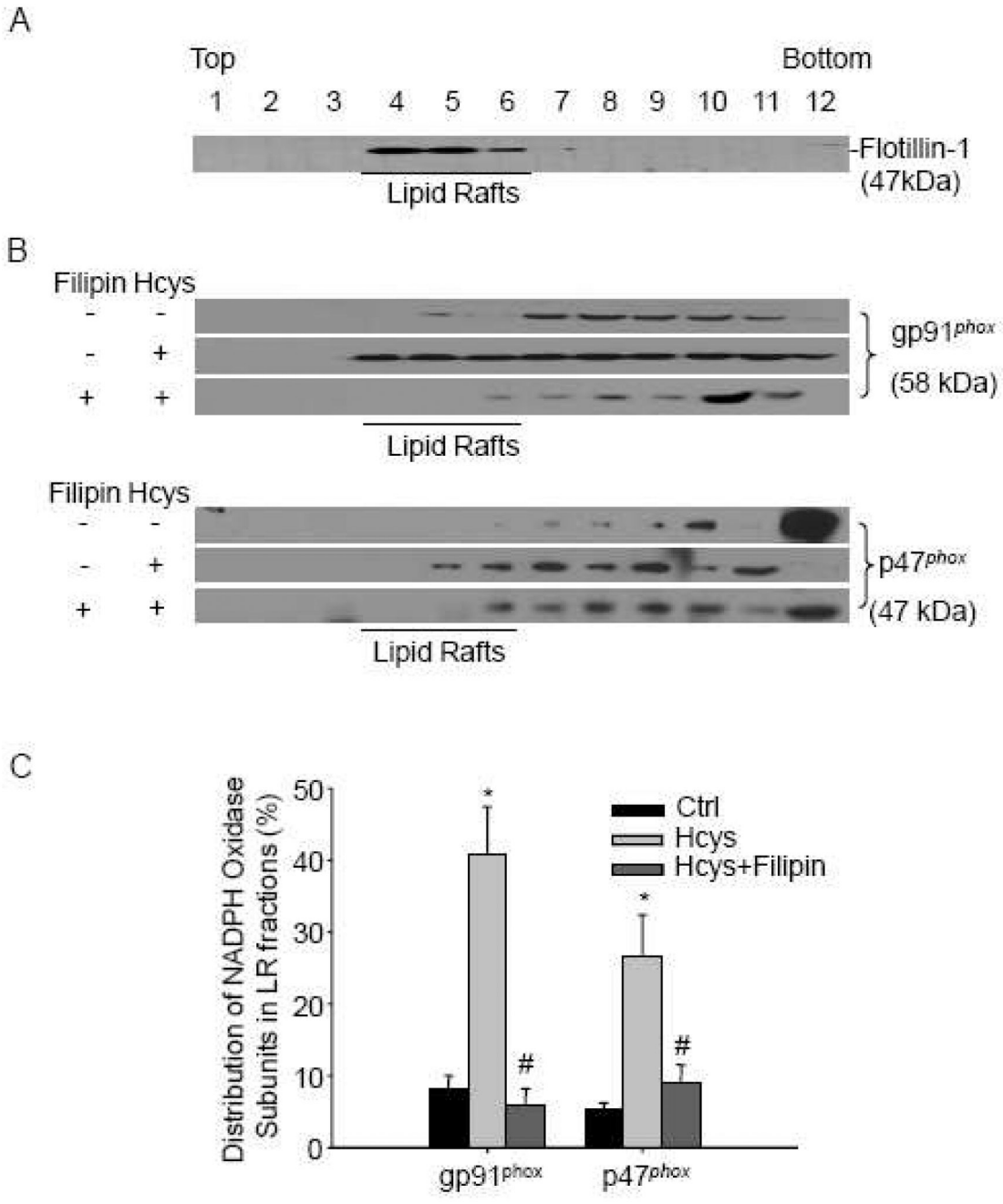

Figure 4. gp91*phox* and p47*phox* are enriched in isolated LR fractions upon Hcys stimulation

A: Podocytes were treated with Hcys (80 μM, 30min) alone or with a 30 min pretreatment of filipin (1 μg/ml). Numbers (1–12) on the top indicate membrane fractions isolated by gradient centrifugation from the top to bottom. Fractions 1–3 were very light fractions without proteins. Fractions 4–6 were light fractions designated as LR fractions as indicated by detection of the LR marker protein, flotillin-1. Other fractions from 7–12 were usually designated as non-raft fractions including membrane and cytosolic proteins. B: Densitometric analysis of the ratio of gp91*phox* or p47*phox* in LR fractions to the total amount (LR/Total). n=5. * *P*<0.05 vs. control; # *P* 0.05 vs. Hcys.

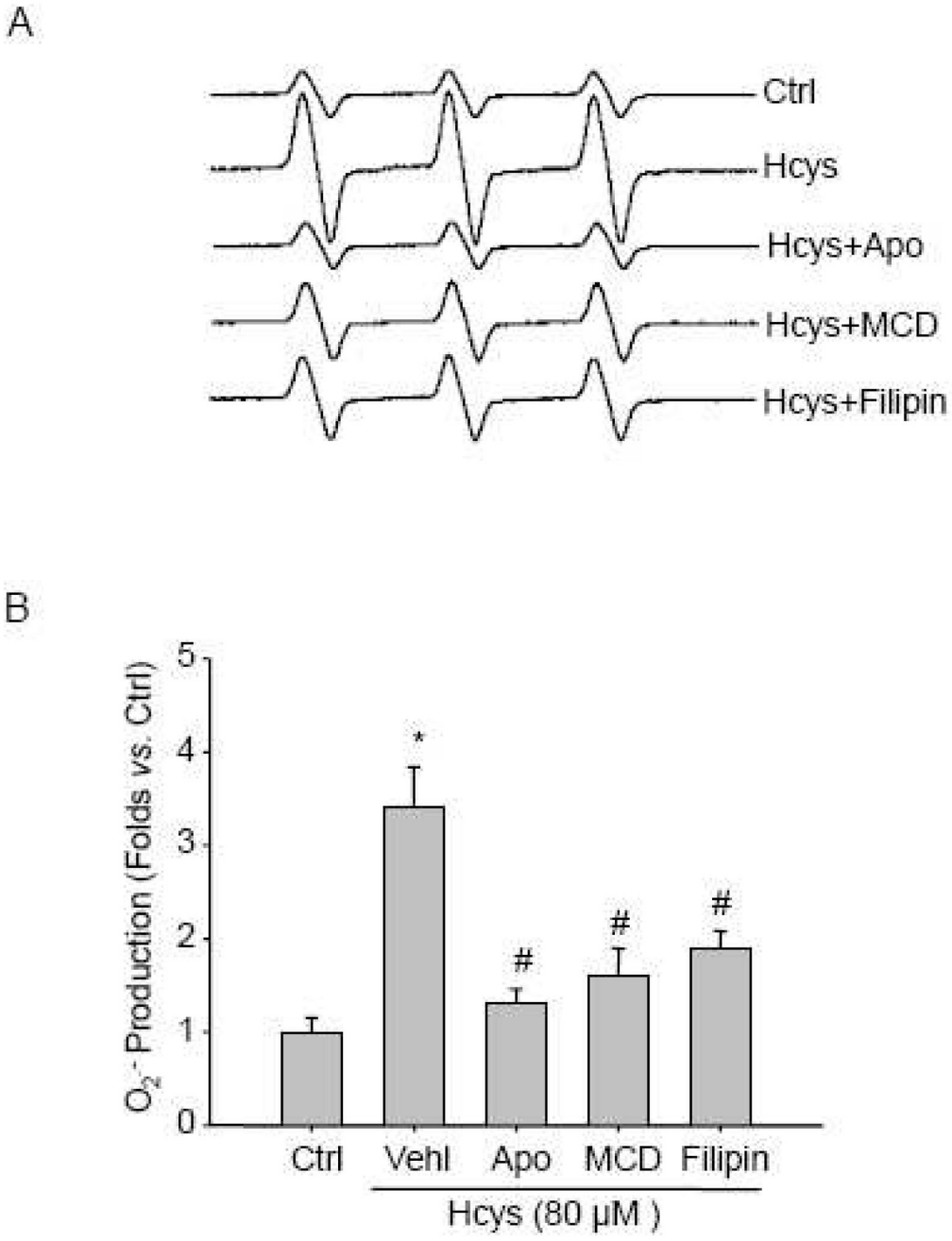

Figure 5. NADPH oxidase inhibitor and LR disruptors inhibit Hcys-induced O_2^{-} production as detected by ESR analysis

A. Representative ESR spectra traces in different groups. B. Summarized data shows the fold changes as compared with control group. Ctrl: control; Vehl: vehicle; Apo: apocynin. n=5. * $P<0.05$ vs. control; # $P<0.05$ vs. Hcys.

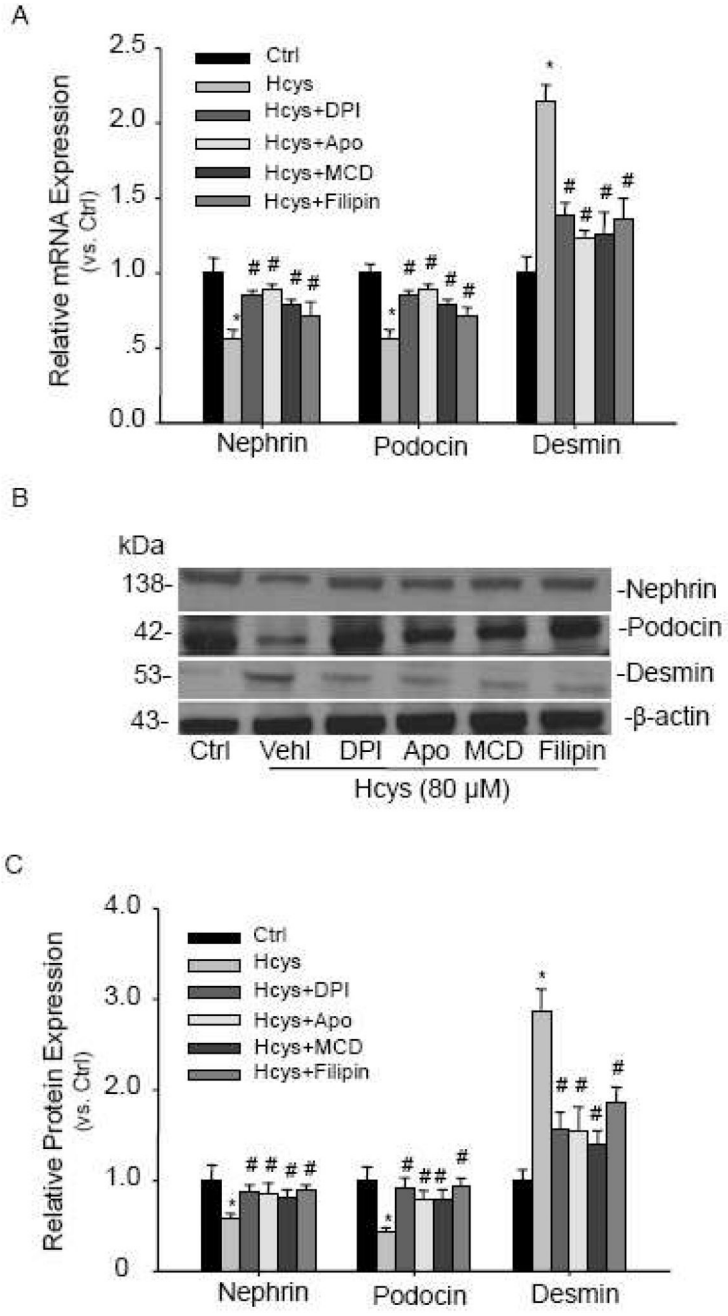

Figure 6. NADPH oxidase inhibitors and LR disruptors restore expression of nephrin, podocin, and desmin altered by Hcys

A. Real-time RT-PCR detection of nephrin, podocin, and desmin mRNA expression induced by Hcys (12 h) in the absence or presence of NADPH oxidase inhibitors (DPI and apocynin) and LR disruptors. n=5. B. Western blot analysis of nephrin, podocin, and desmin protein expression after the cells were incubated with Hcys for 24 h. C. Relative quantitation of protein expression for Western blot analysis. n=5. Ctrl: control; Vehl: vehicle; Apo: apocynin. * $P<0.05$ vs. control; # $P<0.05$ vs. Hcys.

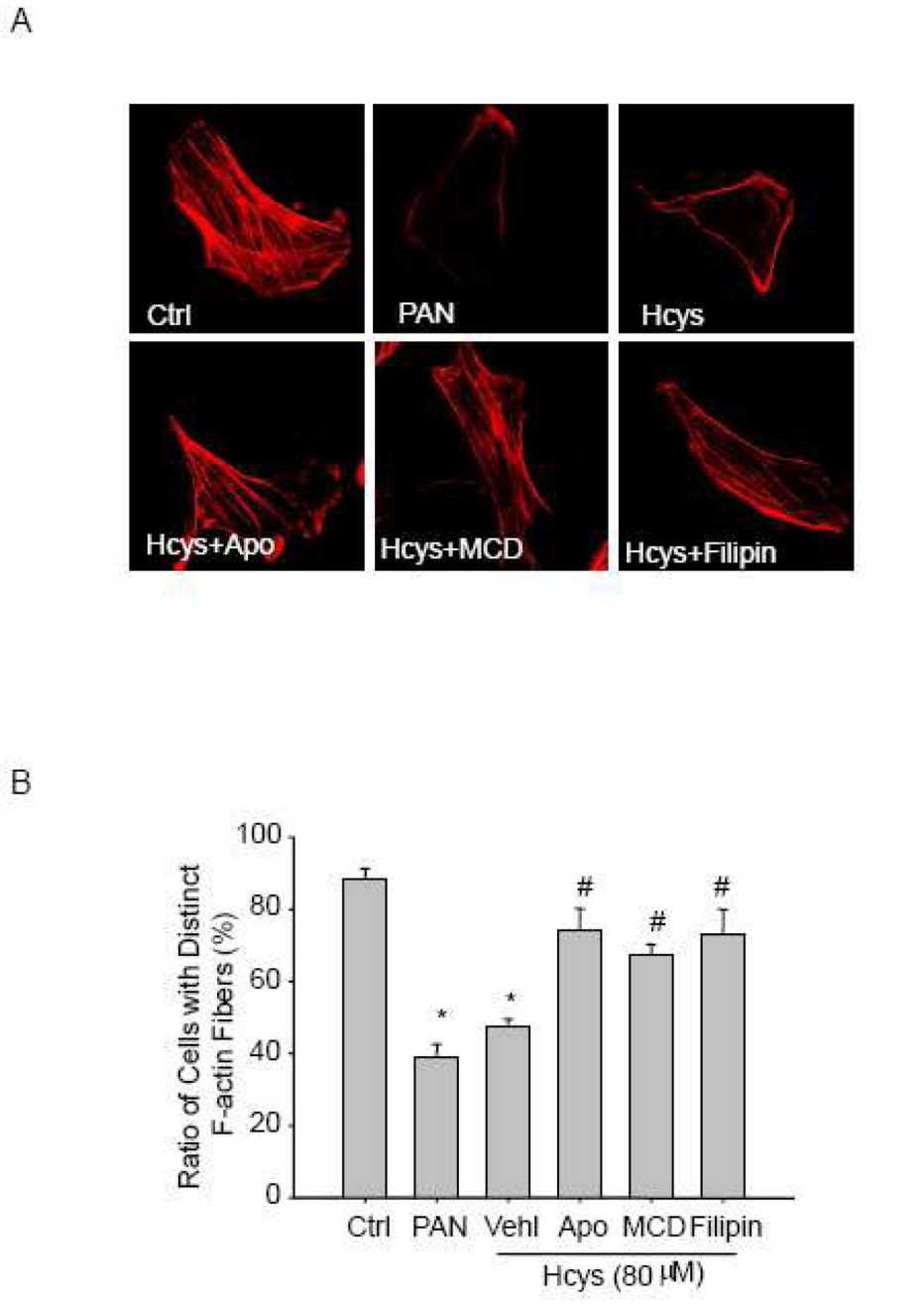

Figure 7. NADPH oxidase inhibitor and LR disruptors recover Hcys-induced actin cytoskeleton disarrangement in podocytes

A. Representative microscopic images of F-actin using rhodamine-phalloidin staining (Original magnification, ×1000). Ctrl: control; Vehl: vehicle; Apo: apocynin. B. Summarized data shows the ratio of podocytes retaining distinct longitudinal stress fibers. Scoring is from100 podocytes on each slide in different groups (n=6). * $P<0.05$ vs. control; # $P<0.05$ vs. Hcys.

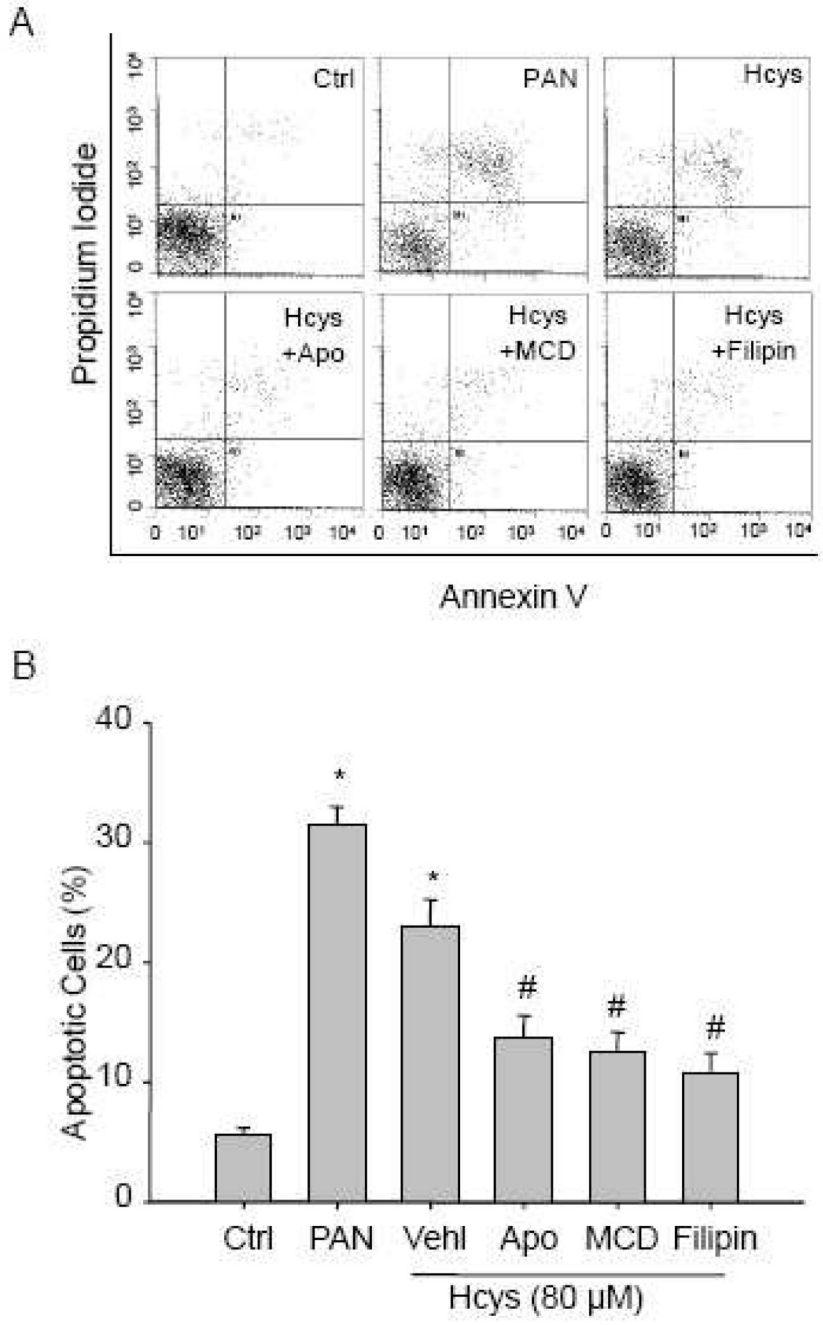

Figure 8. NADPH oxidase inhibitor and LR disruptors attenuate Hcys-induced podocyte apoptosis

A. Flow cytometric recording shows the apoptosis rate of podocytes. Cells in the upper-right and lower-right were considered as apoptotic cells. B. Summarized data shows the rate of apoptotic cells as detected by flow cytometry (n=6). Ctrl: control; Vehl: vehicle; Apo: apocynin. * $P<0.05$ vs. control; # $P<0.05$ vs. Hcys